Comparison of Reconstruction Algorithms for Medical Images

Teresa Chun, Najia Mustafa, Billy Qiu
Department of Electrical and Computer Engineering
University of Waterloo
Waterloo, Ontario

***Abstract*—This paper presents an experimental study comparing various algorithms for medical image reconstruction. In Experiment 1, we focus on MRI-like image reconstruction using the Two-step Iterative Shrinkage/Thresholding (TwIST), Sparse Reconstruction by Separable Approximation (SpaRSA), Fast Iterative Shrinkage-Thresholding Algorithm (FISTA), and Split Augmented Lagrangian Shrinkage Algorithm (SALSA), analyzing their performance in terms of iterations, computational time, Mean Squared Error (MSE), and Structural Similarity Index (SSIM). Experiment 2 involves image deblurring of an actual brain image affected by motion blur and Gaussian noise, evaluating the TwIST, SpaRSA, FISTA, and SALSA algorithms based on CPU time, iterations, MSE, Inverse Signal-to-Noise Ratio (ISNR), and Structural Similarity Index (SSIM). The results demonstrate the efficacy of these algorithms in addressing real-life challenges encountered in medical imaging applications.**

Keywords **Image reconstruction, denoising, image deblurring, TwIST, SpaRSA, FISTA SALSA, MRI, medical imaging, brain image, computational imaging, signal processing, key metrics, MSE, SSIM**

I. Introduction

Advancements in technology have greatly improved the medical field and increased life expectancy over the past decade. Image reconstruction technology, especially in medical imaging, has evolved significantly. With the advent of artificial intelligence (AI) and deep learning, technology's impact on medicine is expected to further escalate [1]. Current research focuses on model-based image reconstruction (MBIR) for CT, MRI, and PET scans to minimize image artifacts and enhance diagnostic accuracy. MBIR also offers the potential to reduce radiation exposure during MRI scans, mitigating long-term risks for patients [2]. However, adopting MBIR for medical images reconstruction poses challenges due to the significant time and computational resources required to develop accurate solutions [2]. Physicians are advised to balance optimization precision with solution convergence time [2].

This study compares the computational efficiency and accuracy of several algorithms for medical image reconstruction:

- Two-step Iterative Shrinkage/Thresholding Algorithm (TwIST)
- Sparse Reconstruction by Separable Approximation Algorithm (SpaRSA)
- Fast Iterative Shrinkage-Thresholding Algorithm (FISTA)
- Split Augmented Lagrangian Shrinkage Algorithm (SALSA)

II. Literature Review

The algorithms for image reconstruction used in our comparison is explained below.

A. Two-step Iterative Shrinkage/ Thresholding Algorithm (TwIST)

The TwIST algorithm is derived from general shrinkage and thresholding algorithms in the field of optimization and signal processing. The algorithm defines a solution (e.g., a restored image) by minimizing the following objective function

$$f(x) = \frac{1}{2} \|y - Kx\|^2 + \lambda\Phi(x)) \tag{1}$$

Where $K : X \to Y$ is the linear direct operator, X and Y are the real Hilbert spaces, $\Phi : X \to \bar{\mathbb{R}}$ is a regularizing function, and λ is the regularization parameter. $\Phi(x)$ can also be defined as the degree of undesirability. [3]

The distinguishing feature of the TwIST algorithm is that each iterate depends on the two previous iterates, rather than only the previous one. The algorithm therefore exhibits a much faster convergence rate than the previously proposed IST algorithm.

B. Sparse Reconstruction by Separable Approximation Algorithm (SpaRSA)

SpaRSA is an optimization algorithm used in the application of solving sparse reconstruction problems. The algorithm solves unconstrained optimization problems of the form

$$\min_x \phi(x) := f(x) + \tau c(x) \tag{2}$$

where $f : \mathbb{R}^n \to \mathbb{R}$ is a smooth function and $c : \mathbb{R}^n \to \mathbb{R}$ is a non-smooth and possibly also non-convex regularization function. SPARSA's strengths lie

in its approach to handling the non-smooth $c(x)$ function using a technique called separable approximation. This approach breaks down the main problem into a sum of smaller subproblems, allowing each subproblem to be solved efficiently at each iteration. [4]

For a sequence of iterates $\{x^t, t = 0, 1, ...\}$, the following subproblem is set up to be solved at each iteration:

$$\mathbf{x}^{t+1} \in \arg\min_{\mathbf{z}} (\mathbf{z}-\mathbf{x}^t) + \frac{\alpha_t}{2} \left\|\mathbf{z}-\mathbf{x}^t\right\|_2^2 + \tau c(\mathbf{z}), \alpha_t \in \mathbb{R}^+ \tag{3}$$

Where z is the objective function on hand. [4]

SPARSA is well-suited for scenarios where the measurements are limited or incomplete, allowing for the reconstruction of high-quality images from sparse data representations.

C. Fast Iterative Shrinkage-Thresholding Algorithm (FISTA)

The FISTA (Fast Iterative Shrinkage-Thresholding Algorithm) is a gradient-based optimization method that improves upon ISTA (Iterative Shrinkage-Thresholding Algorithm) by introducing a momentum term t_k [5].

Given $L = L(f)$, the Lipschitz constant of ∇f, the FISTA algorithm initializes:

$$y_1 = x_0 \in \mathbb{R}^n, \quad t_1 = 1$$

Iterative steps are computed as:

$$x_k = p_L(y_k), \quad t_{k+1} = \frac{1 + \sqrt{1 + 4t_k^2}}{2}, \tag{4}$$

$$y_{k+1} = x_k + \left(\frac{t_k - 1}{t_{k+1}}\right)(x_k - x_{k-1}) \tag{5}$$

where $x_k \in \mathbb{R}^n$: Current iterate at iteration k. $y_k \in \mathbb{R}^n$: Auxiliary variable for computing next iterate. t_k: Momentum parameter for accelerating convergence.$p_L(y_k)$: Iterative shrinkage operator applied to y_k.

In image reconstruction, FISTA recovers $x \in \mathbb{R}^n$ from measurements $y \in \mathbb{R}^m$ by solving:

$$\min_x \ f(x) + g(x)$$

where: - $f(x)$ measures mismatch with y. - $g(x)$ promotes image properties (e.g., sparsity).

Steps:

1) Initialization: x_0 guess, $y_1 = x_0$, $t_1 = 1$.
2) Updates:
   a) x_k minimizes $f(x)$ with $\frac{1}{2\alpha}\|x - y_k\|^2$.
   b) t_{k+1} update.
   c) y_{k+1} update using x_k, x_{k-1}, t_k, t_{k+1}.
3) Iterate until convergence.

FISTA efficiently reconstructs images from noisy or undersampled data, with parameter tuning optimizing results.

D. Split Augmented Lagrangian Shrinkage Algorithm (SALSA)

Afonso et al. introduced SALSA (Split Augmented Lagrangian Shrinkage Algorithm) for image reconstruction, involving split variables and augmented Lagrangian integration [6]. The algorithm aims to solve:

$$\min_{u,v} f_1(u) + f_2(v) \quad \text{s.t.} \quad g(u) = v \tag{6}$$

where u and v are split variables, and $f_1(u)$, $f_2(v)$, and $g(u)$ are components of the optimization problem.

The augmented Lagrangian L_A is defined as:

$$L_A(z, \lambda, \mu) = E(z) + \lambda^T(b - Hz) + \frac{\mu}{2}\|Hz - b\|_2^2 \tag{7}$$

where z is the optimization variable, λ is the vector of Lagrange multipliers, and μ is the penalty parameter.

SALSA leverages ADMM (Alternating Direction Method of Multipliers) and ALM (Augmented Lagrangian Method) to update variables iteratively, performing image recovery via unconstrained optimization:

$$f_1(x) = \frac{1}{2}\|Ax - y\|_2^2, \quad f_2(x) = \tau\phi(x), \quad G = I \tag{8}$$

where x is the input image, A is the system matrix, y is the corrupted image, $\phi(x)$ is a regularization function, and τ is the regularization parameter. ADMM combines dual ascent with proximal methods to efficiently solve constrained convex optimization problems.

III. Experiment

The MATLAB implementation of algorithms described in [6] and [7] by Afonso, Bioucas-Dias, and Figueiredo were utilized for image recovery in the experiments.

A. Experimental Setup for Experiment 1 (MRI-like Image Reconstruction)

1) **Image Generation:** A custom MRI-like image resembling the Shepp-Logan phantom was generated with dimensions 128×128 pixels.
2) **Observations:** Gaussian noise with a standard deviation of 1×10^{-3} was added to the acquired data to simulate realistic noise levels in MRI scans.

Parameters Used for Each Algorithm in Experiment 1:

- **TwIST:**
  - Regularization parameter (λ) was set to 9×10^{-5}. Stopping criterion was set to 3, indicating convergence based on the change in the objective function.
- **SpaRSA:**
  - Regularization parameter (λ) was set to match the objective value of TwIST. Stopping criterion was set to 4, indicating convergence based on the change in the objective function.

- **FISTA:**
  - Regularization parameter (λ) was set to match the objective value of TwIST. Maximum number of iterations was set to 500.
- **SALSA:**
  - Mu parameter was set to λ multiplied by 100. Maximum number of iterations was set to 1000.

Evaluation Metrics Used in Experiment 1:

- **Mean Squared Error (MSE):** Measures the average squared difference between the estimated image and the ground truth. The Mean Squared Error (MSE) is calculated using the formula:

$$\text{MSE} = \frac{1}{mn}\sum_{i=1}^{m}\sum_{j=1}^{n}(I(i,j) - \hat{I}(i,j))^2 \quad (9)$$

  $I(i,j)$ and $\hat{I}(i,j)$ are the pixel values of the ground truth image and the estimated image at location (i,j), respectively. m and n are the dimensions (height and width) of the images.
- **Structural Similarity Index (SSIM):** Quantifies the similarity between two images based on luminance, contrast, and structure. The Structural Similarity Index (SSIM) is computed as [8]:

$$\text{SSIM}(I,\hat{I}) = \frac{(2\mu_I\mu_{\hat{I}} + c_1)(2\sigma_{I\hat{I}} + c_2)}{(\mu_I^2 + \mu_{\hat{I}}^2 + c_1)(\sigma_I^2 + \sigma_{\hat{I}}^2 + c_2)} \quad (10)$$

μ_I and $\mu_{\hat{I}}$ are the means of images I and $\hat{I}$, respectively. σ_I^2 and $\sigma_{\hat{I}}^2$ are the variances of images I and $\hat{I}$, respectively. $\sigma_{I\hat{I}}$ is the covariance between I and $\hat{I}$. c_1 and c_2 are constants to stabilize the division with weak denominator (to avoid instability near zero).

Rationale for Experimental Design: The decision to use a small-scale demo for Experiment 1 was driven by the need to showcase the fundamental capabilities of the algorithms in a controlled environment.

The original and noisy MRI-like images for Experiment 1 are shown in Figures 1 and 2 respectively.

Fig. 1: Original MRI-like Image

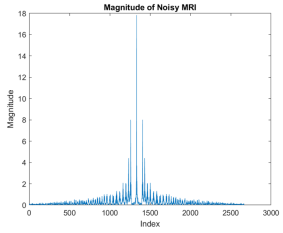

Fig. 2: Magnitude of Noisy MRI-like Image

B. Experimental Setup for Experiment 2 (Real Brain Image Reconstruction):

1) **Original Image:** An actual brain image [9] of size 512×512 pixels.
2) **Blur Model:** A 4×4 uniform blur kernel was applied to the original image to simulate motion blur.
3) **Observations:** Gaussian noise with a Signal-to-Noise Ratio (SNR) of 45 dB was added to the blurred image to simulate noise commonly encountered in imaging systems.

Parameters in Experiment 2:

Same parameters as Experiment 1 except the regularization parameter was set to 2×10^{-2}

Evaluation Metrics Used in Experiment 2:

- **Mean Squared Error (MSE)**
- **Structural Similarity Index (SSIM)**

Rationale for Experimental Design: The decision to conduct a experiment with an actual brain image for Experiment 2 was motivated by the need to assess algorithm performance in more challenging and realistic conditions. This allowed for the evaluation of algorithm robustness, scalability, and effectiveness in handling real-world data complexities.

The original and noisy brain images for Experiment 2 are shown in Figures 3 and 4 respectively.

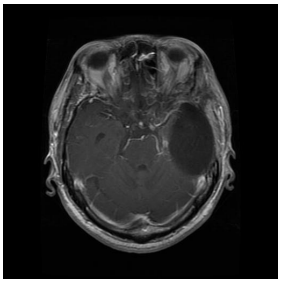

Fig. 3: Original Image

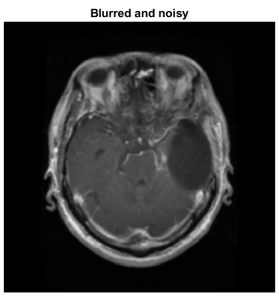

Fig. 4: Noisy Image

IV. Results

The results of both Experiment 1 (MRI-like Image Reconstruction) and Experiment 2 (Real Brain Image Reconstruction) are presented in Tables I and II respectively.

A. Experiment 1: MRI-like Image Reconstruction

TABLE I: Results for Experiment 1

Algorithm	CPU Time (s)	MSE	SSIM
TwIST	100.766	6.86856×10^{-7}	0.99937
SpaRSA	161.391	0.000198925	0.834662
FISTA	92.9062	4.66974×10^{-7}	0.999591
SALSA	41.8438	1.06247×10^{-6}	0.998651

B. Experiment 2: Real Brain Image Reconstruction

TABLE II: Results for Experiment 2:

Algorithm	CPU Time (s)	MSE	SSIM
TwIST	3.56×10^3	2.86	0.92341
SpaRSA	1.79×10^4	4.11	0.915329
FISTA	781	4.11	0.916691
SALSA	447	2.64	0.908621

The reconstructed brain images from the four algorithms are shown below in Figure 5

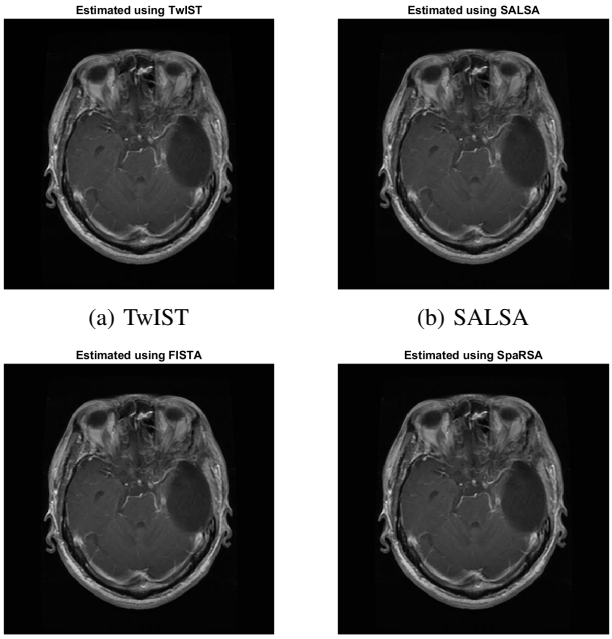

(a) TwIST (b) SALSA

(c) FISTA (d) SpaRSA

Fig. 5: Reconstructed Brain Images

V. Analysis

The performance of various algorithms in Experiment 1 is evaluated based on convergence characteristics, computational efficiency, and the quality of MRI-like image reconstruction.

- **TwIST**: The TwIST algorithm demonstrates moderate convergence. The resulting Mean Squared Error (MSE) is remarkably low, indicating high fidelity in reconstructing the MRI-like image. Additionally, the Structural Similarity Index (SSIM) of 0.99937 indicates a very close resemblance to the original image in terms of luminance, contrast, and structure.
- **SpaRSA**: SpaRSA requires a substantial CPU time to achieve convergence. The SSIM value of 0.834662 indicates that while SpaRSA produces a reasonable reconstruction, it may not fully preserve finer details and structures present in the original image.
- **FISTA**: FISTA achieves convergence with a CPU time of 92.9062 seconds, which is relatively efficient compared to SpaRSA. The MSE is exceptionally low, suggesting high accuracy in image reconstruction. The SSIM value of 0.999591 indicates excellent similarity with the ground truth.
- **SALSA**: SALSA demonstrates efficient convergence with a short CPU time of 41.8438 seconds. Despite its rapid execution, SALSA achieves a low MSE and a high SSIM value of 0.998651, indicating high reconstruction fidelity and similarity with the original image.

The results from Experiment 2 provide insights into the performance of different algorithms for a real brain image deblurring. Here's a breakdown of the findings:

- **TwIST** achieved a relatively low Mean Squared Error (MSE) of 2.86. The Structural Similarity Index (SSIM) of the estimated image compared to the ground truth was 0.92341.
- **SpaRSA** required significantly longer computation time (1.79×10^4 seconds) compared to other algorithms, with a higher MSE of 4.11 . The SSIM value was 0.915329.
- **FISTA** demonstrated a comparable performance to SpaRSA in terms of MSE, with a shorter runtime of 781 seconds. The SSIM was 0.916691.
- **SALSA** offered a good balance between computation time and MSE. It achieved an MSE of 2.64, with an SSIM of 0.908621.

VI. Conclusion

The comparison of algorithm performance in both Experiment 1 (MRI-like image reconstruction) and Experiment 2 (Actual Brain Image Deblurring) provides insights into their effectiveness across different imaging scenarios. TwIST and FISTA showed efficient convergence with low MSE and high SSIM, indicating superior reconstruction fidelity. SpaRSA, while effective, required more computational resources and exhibited slightly lower fidelity. SALSA demonstrated rapid convergence and high reconstruction quality. Overall, TwIST and FISTA consistently outperformed SpaRSA in reconstruction quality and computational efficiency. SALSA offers promise for real-time applications due to its rapid convergence and good reconstruction fidelity.

REFERENCES

[1] James S. Duncan, Michael F. Insana, and Nicholas Ayache. Biomedical imaging and analysis in the age of big data and deep learning [scanning the issue]. *Proceedings of the IEEE*, 108(1):3–10, 2020.

[2] Jingyan Xu and Frédéric Noo. Convex optimization algorithms in medical image reconstruction—in the age of ai. *Physics in Medicine & Biology*, 67(7):07TR01, 2022.

[3] JosÉ M. Bioucas-Dias and MÁrio A. T. Figueiredo. A new twist: Two-step iterative shrinkage/thresholding algorithms for image restoration. *IEEE Transactions on Image Processing*, 16(12):2992–3004, 2007.

[4] Stephen J. Wright, Robert D. Nowak, and MÁrio A. T. Figueiredo. Sparse reconstruction by separable approximation. *IEEE Transactions on Signal Processing*, 57(7):2479–2493, 2009.

[5] Amir Beck and Marc Teboulle. A fast iterative shrinkage-thresholding algorithm with application to wavelet-based image deblurring. In *2009 IEEE International Conference on Acoustics, Speech and Signal Processing*, pages 693–696, 2009.

[6] M. Afonso, J. Bioucas-Dias, and M. Figueiredo. Fast image recovery using variable splitting and constrained optimization. *IEEE Transactions on Image Processing*, 19(9):2345–2356, September 2010.

[7] M. Afonso, J. Bioucas-Dias, and M. Figueiredo. An augmented lagrangian based method for the constrained formulation of imaging inverse problems. *IEEE Transactions on Image Processing*, 20(3):681–695, March 2011.

[8] Z. Wang, A. C. Bovik, H. R. Sheikh, and E. P. Simoncelli. Image quality assessment: From error visibility to structural similarity. *IEEE Transactions on Image Processing*, 13(4):600–612, 2004.

[9] Msoud Nickparvar. Brain tumor mri dataset, 2021.